IET Microwaves, Antennas & Propagation

Research Article

IET Journals
The Institution of Engineering and Technology

Ninja array antenna: novel approach for low backscattering phased array antenna

ISSN 1751-8725
Received on 11th June 2017
Revised 11th October 2017
Accepted on 25th October 2017
doi: 10.1049/iet-map.2017.0496
www.ietdl.org

Keisuke Konno[1] ✉, *Qiaowei Yuan*[2], *Qiang Chen*[1]

[1]*Department of Communications Engineering, Tohoku University, Sendai, Japan*
[2]*National Institute of Technology, Sendai College, Sendai, Japan*
✉ *E-mail: konno@ecei.tohoku.ac.jp*

Abstract: This study presents a novel concept of a low backscattering phased array antenna, a Ninja array antenna. One of the advantages of the Ninja array antenna over the conventional phased array antenna is low backscattering performance over its operating frequency band, which is not available using a conventional phased array antenna with a band-pass radome. The Ninja array antenna is designed in the same manner as the design of reflectarrays, so that the main lobe of its scattering field is directed to a specific direction except for backscattering one. As a result, its backscattering is reduced in comparison with that of the conventional phased array antenna. Although the Ninja array antenna is composed of non-identical array elements such as the reflectarray, it works as a phased array antenna because desired amplitude and phase of excitation can be obtained numerically via an array element pattern. Numerical simulation is performed and the scattering/radiation performance of the Ninja array antenna is demonstrated.

1 Introduction

A phased array antenna has received much attention over several decades [1–3]. Usually, most of the phased array antenna is a periodic array antenna and is composed of hundreds or thousands of identical array elements. As a result, backscattering of the phased array antenna can be quite large. It is challenging to reduce the backscattering of the phased array antenna and extensive efforts have been dedicated.

A radome is one of the effective approaches to reduce the backscattering of the phased array antenna. A band-pass radome which is composed of a frequency selective surface (FSS) is a popular technique in order to reduce the backscattering of the phased array antenna [4, 5]. The band-pass radome is expected to be transparent in the operating frequency band of the phased array antenna in order not to prevent its operation. On the other hand, the band-pass radome is expected to be opaque in the other frequency band and its backscattering is expected to be as small as possible. Transmission performance of an A-sandwich radome with a conducting wire at its junctions has been clarified [6]. A miniature conical thick-screen FSS radome at C band and an FSS radome which is able to absorb an incident wave above its transmission band have been proposed, respectively [7, 8]. These band-pass radomes are able to mitigate the backscattering of the phased array antenna out of its operating frequency band. However, backscattering of the phased array antenna is remaining high in its operating frequency band even when the phased array antenna is covered by the band-pass radome.

Radar absorbing materials (RAM) are another promising techniques in order to reduce the backscattering of the phased array antenna. Resistive sheet type absorbers have been proposed for microwave or millimeter wave bands [9, 10]. Microstructures of a multineedle zinc oxide whisker and multilayer plasma stealth structure have been proposed [11, 12]. Disadvantage of the RAM is to absorb not only an incoming wave but also an outgoing wave from the phased array antenna. Resultant absorption of the waves leads to degradation of the performance of the phased array antenna. Moreover, energy dissipation from the RAM can be a serious problem because the phased array antenna deals with high power.

Randomness has been used in order to reduce the backscattering of scatterers [13, 14]. The backscattering of the phased array antenna covered by randomly distributed scatterers is expected to be reduced in its operating frequency band when these scatterers are well designed. However, an outgoing wave from the phased array antenna is blocked. To the best of our knowledge, a phased array antenna whose backscattering is quite small in its operating frequency band while keeping its performance as the phased array has not been proposed.

In this paper, a novel approach for a low backscattering phased array antenna is proposed. Authors call the proposed antenna 'Ninja array antenna', where Ninja is a traditional covert agent who works stealthily in Japan. The Ninja array antenna is composed of non-identical array elements. Dimensions of each array element are adopted in order to reduce the backscattering of the phased array while keeping its radiation performance. Small backscattering performance of the Ninja array antenna is designed in analogous to reflectarray [15–17]. Excitations of non-identical array elements are obtained using their array element patterns. The performance of the proposed array antenna is demonstrated via numerical simulations.

2 Design of Ninja array antennas

The Ninja array antenna should be designed not only as a radiator but also as a scatterer. Therefore, an antenna element which has multiple degree of freedom for design is preferable as an array element, e.g. an antenna with parasitic elements or a multimode antenna.

As a radiator, each antenna element must be terminated by a load impedance and its active impedance should be close to 50 Ω over its operating frequency band. For example, for the antenna with parasitic elements, the length of feeding element should be designed in advance and the remaining degree of freedom should be used for design of its scattering performance because the length of feeding element strongly affects its active impedance.

In terms of scattering performance, the Ninja array antenna is a reflectarray. Therefore, it is designed as follows as a reflectarray.

i. Centre frequency and mainbeam direction of the scattering field (θ_s, ϕ_s) for the Ninja array antenna are given previously.
ii. At the centre frequency, a reflection coefficient $\Gamma(l)$ of a Ninja array element is obtained using numerical simulations such as isolated element approach [18], surrounded element approach [19, 20], or periodic boundary conditions [21–23]

$$\Gamma(l) = \frac{E(\theta_s, \phi_s)}{E(\theta_i, \phi_i)}, \quad (1)$$

iii. where (θ_i, ϕ_i) is an incident angle of plane wave, and l the dimension of the Ninja array element under simulation.
iv. The dimension of a reference Ninja array element can be determined arbitrarily.
v. Using $\Gamma(l)$ multiplied by an array factor, the dimensions of the other Ninja array elements are obtained in order to form the mainbeam directed to (θ_s, ϕ_s).

The designed Ninja array is a periodic array which is composed of non-identical elements and its scattering performance can be obtained using method of moments (MoM) [24, 25].

2.1 Excitations of non-identical array elements

An excitation of every element must be given to steering the non-identical array elements because the Ninja array antenna is operating as a phased array antenna. Here, the excitation of every element is obtained via array element patterns obtained using the MoM.

A linear system obtained using the MoM is expressed as follows:

$$\boldsymbol{V} = \boldsymbol{Z}\boldsymbol{I}, \quad (2)$$

where $\boldsymbol{V}$ is the $N \times 1$ excitation vector, $\boldsymbol{I}$ the $N \times 1$ current vector, $\boldsymbol{Z}$ the $N \times N$ impedance matrix, and N the total number of unknowns. Here, all array element currents are obtained from (2)

$$\boldsymbol{I}_m = \boldsymbol{Z}^{-1}\boldsymbol{V}_m, \quad \text{where} \quad m = 1, 2, \ldots, M, \quad (3)$$

where $\boldsymbol{V}_m$ is the $N \times 1$ excitation vector whose entries are only unity at a feeding point of the mth Ninja array element and are zero at elsewhere. $\boldsymbol{I}_m$ is the resultant $N \times 1$ array element current vector. M is the total number of the Ninja array elements and $N = \sum_{m=1}^{M} K_m$, where K_m is the number of unknowns in the mth array element.

After all array element currents are obtained from (3), non-identical array factor (NIAF) is numerically obtained for all Ninja array elements

$$C_m = \frac{E(\theta_r, \phi_r, l_R)}{E(\theta_r, \phi_r, l_m)}, \quad \text{where} \quad m = 1, \ldots, M, \quad (4)$$

where $E(\theta_r, \phi_r, l_R)$ and $E(\theta_r, \phi_r, l_m)$ are array element patterns when a reference and the mth Ninja array element are excited, respectively, and their polarisation is co-polarisation of the Ninja array element. θ_r and ϕ_r are desired main beam direction in elevation and azimuth angle, respectively. l_R and l_m indicate the length of the reference and mth element in the array antenna, respectively. Array element pattern is obtained using the following equation

$$\boldsymbol{E}(\theta_r, \phi_r, l_m) = \frac{e^{-jkr}}{r} \sum_{m=1}^{M} \sum_{k=1}^{K_m} I_k \boldsymbol{D}_k(\theta_r, \phi_r, l_m)\, e^{j\boldsymbol{k}_r \cdot \boldsymbol{r}'_m}, \quad (5)$$

where $\boldsymbol{D}_k$ and I_k are a directivity function and current of the kth segment in the mth element, respectively. $e^{j\boldsymbol{k}_r \cdot \boldsymbol{r}'_m}$ is the so-called array factor. A wavenumber vector $\boldsymbol{k}_r = k_0(\sin\theta_r\cos\phi_r, \sin\theta_r\sin\phi_r, \cos\theta_r)$ and position vector of the mth element $\boldsymbol{r}'_m = (x', y', z')$.

Finally, an excitation vector for the designed Ninja array antenna in order to form a mainbeam directed to (θ_r, ϕ_r) is given as follows:

$$\boldsymbol{V} = \sum_{m=1}^{M} \boldsymbol{V}_m(\theta_r, \phi_r). \quad (6)$$

Here, $\boldsymbol{V}_m(\theta_r, \phi_r)$ is a vector whose entries are C_m at a feeding point of the mth Ninja array element and zero at elsewhere. The resultant excitation vector for the designed Ninja array antenna includes the effects of mutual coupling and current distribution of the entire array. Therefore, our proposed method works in order to obtain the excitation vector for the Ninja array antenna which is composed of a multi-mode element as well as a single-mode element.

3 Numerical examples

It is important to design a moderate array element for the Ninja array antenna. Two types of elements are designed and their performances are numerically demonstrated in this paper. The first one is composed of a Yagi-Uda element [26] and the second one is composed of a log-periodic dipole array (LPDA) element [27–29]. The Yagi-Uda element is well known as a narrowband, single-mode antenna, while the LPDA is well known as a wideband, multi-mode antenna. Fig. 1 shows dimensions of both elements and Ninja array antennas. Dimensions of these Ninja array elements are expected to be over $\lambda/2$ at their operating frequency bands. Therefore, a triangular periodic lattice is introduced to designed planar uniform and Ninja array antennas in order to prevent grating lobes to appear in visible region as much as possible. Numerical simulation was performed using Richmond's MoM and isolated element approach was used in order to obtain reflection coefficients [18, 25].

3.1 Phase of reflection coefficients

Phase of reflection coefficients of the Ninja array elements should be obtained in advance to design the Ninja array antenna as a reflectarray. A couple of numerical simulations were performed in advance and dimensions of Ninja array elements are optimised in order to enhance their phase variations. For example, τ, which is the ratio between the lengths of two adjacent dipole elements, is set to 0.85. The interested readers can refer to [30, 31] in order to know how to design the LPDA element as a scatterer. A 50 Ω resistance is loaded with a feeding point of array elements, which is a different point with an ordinary reflectarray.

The phase of reflection coefficients $\Gamma(l)$ of the Yagi-Uda element and the LPDA element is shown in Figs. 2 and 3, respectively. Here, the phase versus the length of a director l_3 is obtained for the Yagi-Uda element, while the phase versus the length of the shortest dipole l_1 is obtained for the LPDA element. According to Figs. 2 and 3, it is found that the phase variation is over 297° for the Yagi-Uda element and 786° for the LPDA element.

Figs. 2 and 3 imply that the bandwidth of scattering performance of Ninja array antennas with these array elements is different. The phase of reflection coefficient of the Yagi-Uda element shows strong non-linearity while that of the LPDA element is linear. Therefore, a Ninja array antenna with the LPDA element is expected to have wideband scattering performance rather than that of with the Yagi-Uda element.

3.2 Linear Ninja arrays and their performance

In order to demonstrate the proposed design scheme, a 10×1 Ninja array antenna with Yagi-Uda elements are designed at 300 MHz. All array elements are identical except for the length of the director l_3 as shown in Table 1, so that the main beam of the scattering field is directed to $(\theta_s, \phi_s) = (10°, 0)$. Of course, the scattering field of a couple of Yagi-Uda elements may not be in-phase because the phase variation of reflection coefficient of the Yagi-Uda element is not over 360°. Therefore, the dimension of Yagi-Uda elements is adopted, so that their scattering field is close to in-phase as much as possible.

Bistatic radar cross-section (BRCS) patterns of uniform and Ninja array antennas are shown in Fig. 4. It is found that backscattering of the Ninja array is 13.1 dB lower than that of the uniform array because the Ninja array is designed as a reflectarray and is composed of non-identical elements, while the uniform array is composed of identical elements. The actual gain pattern of the

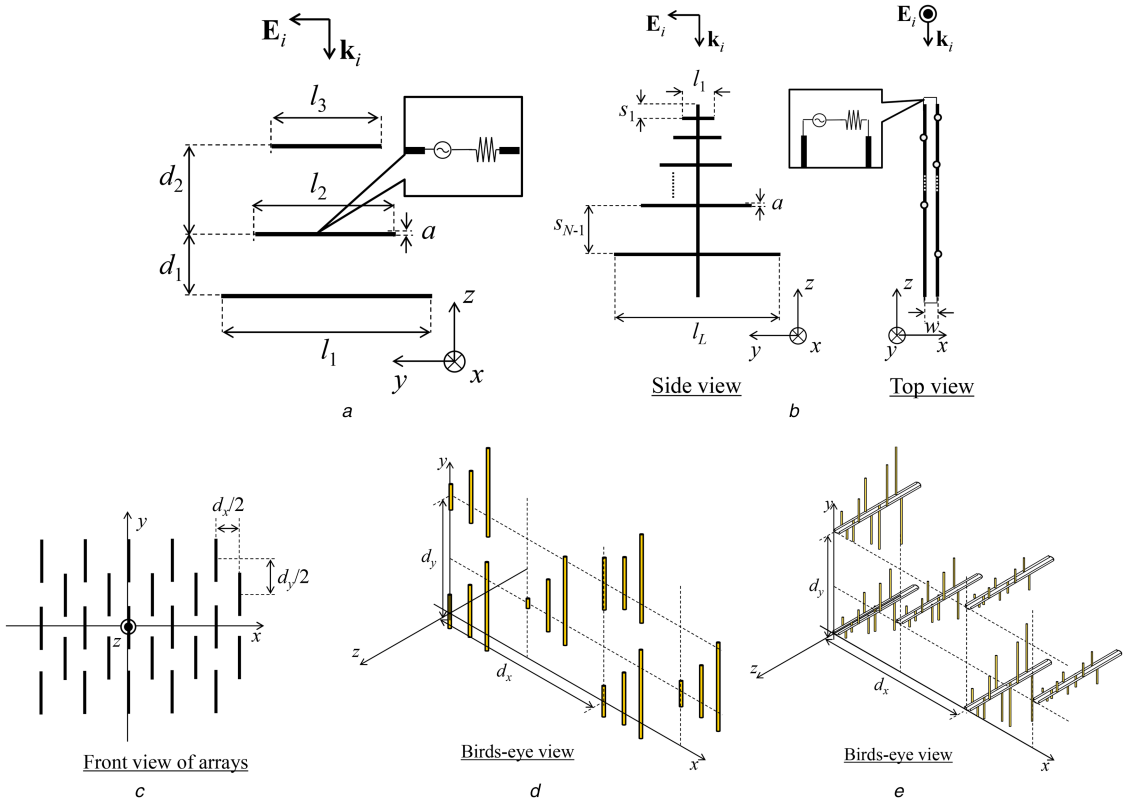

Fig. 1 *Ninja array antennas and their elements*
(a) Yagi-Uda element, ***(b)*** LPDA element, ***(c)*** Front view of Ninja array antennas, ***(d)*** Birds eye view of a Ninja array antenna with Yagi-Uda elements, ***(e)*** Birds eye view of a Ninja array antenna with LPDA elements

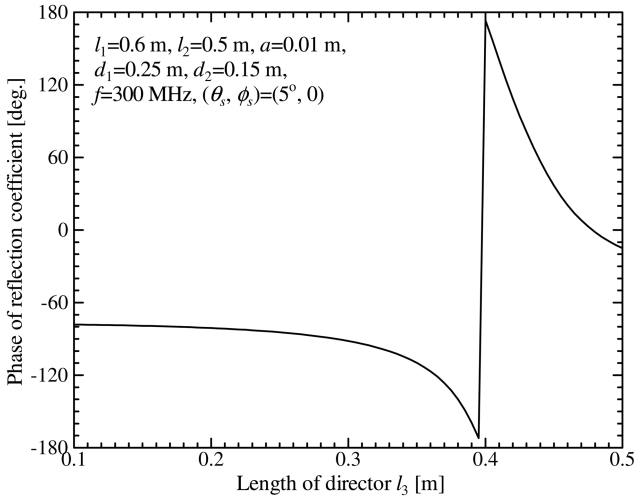

Fig. 2 *Phase of reflection coefficient of an isolated Yagi-Uda element versus* l_3

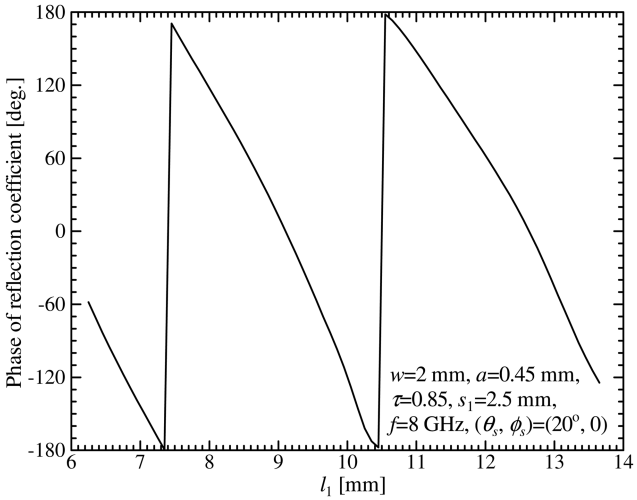

Fig. 3 *Phase of reflection coefficient of an isolated LPDA element versus* l_1

Table 1 Dimensions and excitations of a 10×1 Ninja array antenna with Yagi-Uda elements

Element number	l_3, m	Excitation, V
1 (reference element)	0.1	1
2	0.305	0.89 + j0.04
3	0.375	0.74 + j0.05
4	0.395	0.73 + j0.19
5	0.41	0.81 + j0.26
6	0.425	0.7 + j0.27
7	0.445	0.65 + j0.64
8	0.475	2.06 + j1.33
9	0.5	1.88 + j0.15
10	0.23	0.88−j0.16

designed Ninja array antenna is shown in Fig. 5. Excitation of each array element which is shown in Table 1 is given by (4) and (6), so that main beam of the actual gain pattern is directed to $(\theta_r, \phi_r) = (0, 0)$. It is clearly seen that the main beam of the actual gain pattern is directed to broadside direction, although the excitation of each array element is non-uniform. Therefore, it is concluded that the performance of the proposed design scheme and the Ninja array antenna have been demonstrated.

3.3 Planar Ninja arrays

According to a design scheme shown in Section 2, 10×10 Ninja array antennas are designed. The operating frequency is set to 300 MHz for the Ninja array antenna with the Yagi-Uda element and 8 GHz for the Ninja array antenna with the LPDA element. Directions of the main beam of Ninja array antennas are

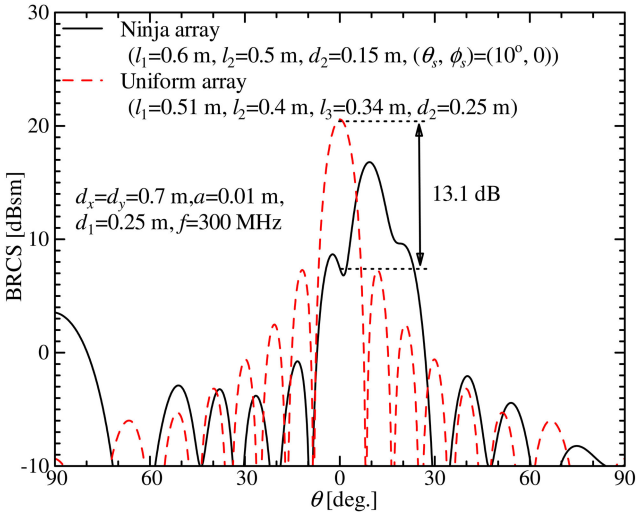

Fig. 4 *BRCSs of* 10×1 *uniform and Ninja array antennas with Yagi-Uda elements (xz-plane,* E_ϕ*, normal incidence)*

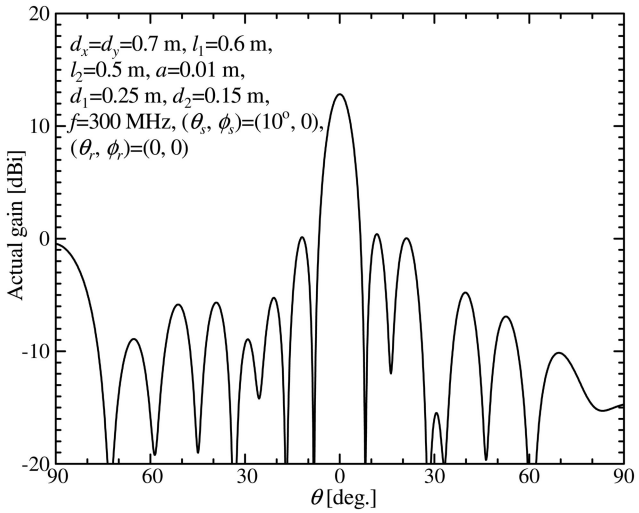

Fig. 5 *Actual gain pattern of a* 10×1 *Ninja array antenna with Yagi-Uda elements (xz-plane,* E_ϕ*)*

$(\theta_s, \phi_s) = (5^\circ, 0)$ for the Ninja array antenna with the Yagi-Uda element and $(\theta_s, \phi_s) = (20^\circ, 0)$ for the Ninja array antenna with the LPDA element. The designed 10×10 Ninja array antennas have triangular periodic structure as shown in Fig. 1.

3.4 Scattering performance

BRCS patterns of uniform and Ninja array antennas are shown in Figs. 6*a* and *b*. All uniform and Ninja array antennas are illuminated by plane wave of normal incidence, i.e. $(\theta_i, \phi_i) = (0, 90^\circ)$ and *y*-polarisation. It is found that the main beam of Ninja array antennas is directed to their desired direction. As a result, backscattering of Ninja array antennas becomes relatively small. On the other hand, the main beam of uniform array antennas is directed to backscattering direction because all elements are identical. As shown in Figs. 6*a* and *b*, the BSCS of the Ninja array antenna with Yagi-Uda element is 8 dB smaller than that of the uniform antenna and the BSCS of the Ninja array antenna with the LPDA element is 17.1 dB smaller than that of the uniform antenna. Therefore, the backscattering cross-sections (BSCS) of Ninja array antennas are much smaller than those of uniform array antennas.

The bandwidth of scattering performance of Ninja array antennas is shown in Figs. 6*c* and *d*. Here, the relative bandwidth of scattering performance is evaluated as follows:

$$\text{Bandwidth} = 200 \times \frac{f_2 - f_1}{f_2 + f_1} \quad (\%), \tag{7}$$

where f_1 and f_2 are the low/high end of the band where the BSCS of Ninja array antennas is 3 dB smaller than that of uniform array antennas. According to (7), the bandwidth of BSCS of the Ninja array antenna with Yagi-Uda element is 48% ($f_1 = 270$ MHz and $f_2 = 440$ MHz). On the other hand, the bandwidth of BSCS of the Ninja array antenna with the LPDA element is over 92% (f_1 is <4 GHz and $f_2 = 10.8$ GHz). Therefore, it can be said that both of Ninja array antennas have a lower backscattering than uniform array antennas over wide frequency band. As expected in Section 3.1, relatively wide bandwidth of the Ninja array antenna with the LPDA element comes from wideband scattering performance of the LPDA element including linear phase shift. The wideband scattering performance of both the LPDA element and a reflectarray with the LPDA element has been described in [30, 31].

3.5 Radiation performance

The performance of the proposed excitation method using the NIAF is numerically demonstrated. Figs. 7*a* and *b* show actual gain patterns of designed Ninja array antennas whose excitation is given by the proposed method. It is found that the proposed excitation method works well for both of the Ninja array antennas. On the other hand, the uniform excitation method approximately works for the Ninja array antenna with Yagi-Uda element but not for that with the LPDA element. The Yagi-Uda element is so-called a single-mode antenna and its current distribution is almost uniform even when the dimension of its director varies. As a result, the uniform excitation method approximately works for the Ninja array antenna with Yagi-Uda elements. However, as shown in Fig. 7*a*, small beam tilt (1.4°) is inevitable when the uniform excitation method is used because the Ninja array antenna is composed of non-identical elements and the proposed excitation method is preferable. On the other hand, the Ninja array antenna with the LPDA element forms no main beam when the uniform excitation method is used. The LPDA element is a kind of a multi-mode element and its current distribution varies as its dimension varies. Therefore, the Ninja array antenna with the non-identical LPDA element must be excited carefully in order to form its main beam directed to desired direction. As shown in Section 2, the proposed excitation method is based on array element patterns. The Ninja array antenna with the resultant excitation voltage forms its main beam directed to desired direction because array element patterns include the current distribution of elements and effect of mutual coupling. In order to show the robustness of the proposed excitation method, Figs. 7*c* and *d* show the beam scanning performance of the Ninja array antennas. It is demonstrated that all main beams of Ninja array antennas are directed to their desired directions without beam tilt.

The bandwidth of radiation performance of Ninja array antennas is demonstrated. Bandwidths of uniform and Ninja array antennas are evaluated by (7). Fig. 6 shows actual gains of uniform and Ninja array antennas with respect to frequency. Here, the excitations of the Ninja array antennas are given using the proposed method every time when frequency varies while those of the uniform arrays are given uniformly. The bandwidth of the Ninja array antenna with the Yagi-Uda element is 32% ($f_1 = 240$ MHz and $f_2 = 330$ MHz) while that of the uniform array antenna is 28% ($f_1 = 280$ MHz and $f_2 = 370$ MHz). The bandwidth of the Ninja array antenna with the LPDA element is 57% ($f_1 = 5.6$ GHz and $f_2 = 10.1$ GHz), while that of the uniform array antenna is 66% ($f_1 = 4.6$ GHz and $f_2 = 9.1$ GHz) (Fig. 8). Therefore, it is found that the bandwidth of the Ninja array antennas is comparable to that of the uniform array antennas. It should be noted that the proposed excitation method greatly contributes to such wideband performance of the Ninja array antenna with the LPDA element because the Ninja array antenna which is uniformly excited only has a poor performance as shown in Fig. 7*b*.

Finally, beam scanning capability of Ninja array antennas is demonstrated in Fig. 9. It is found that beam scanning capability of the Ninja array antennas are comparable to that of the uniform array antennas. For the uniform and Ninja array antenna with LPDA elements, grating lobe appears at $\theta_r > 30^\circ$ and the maximum

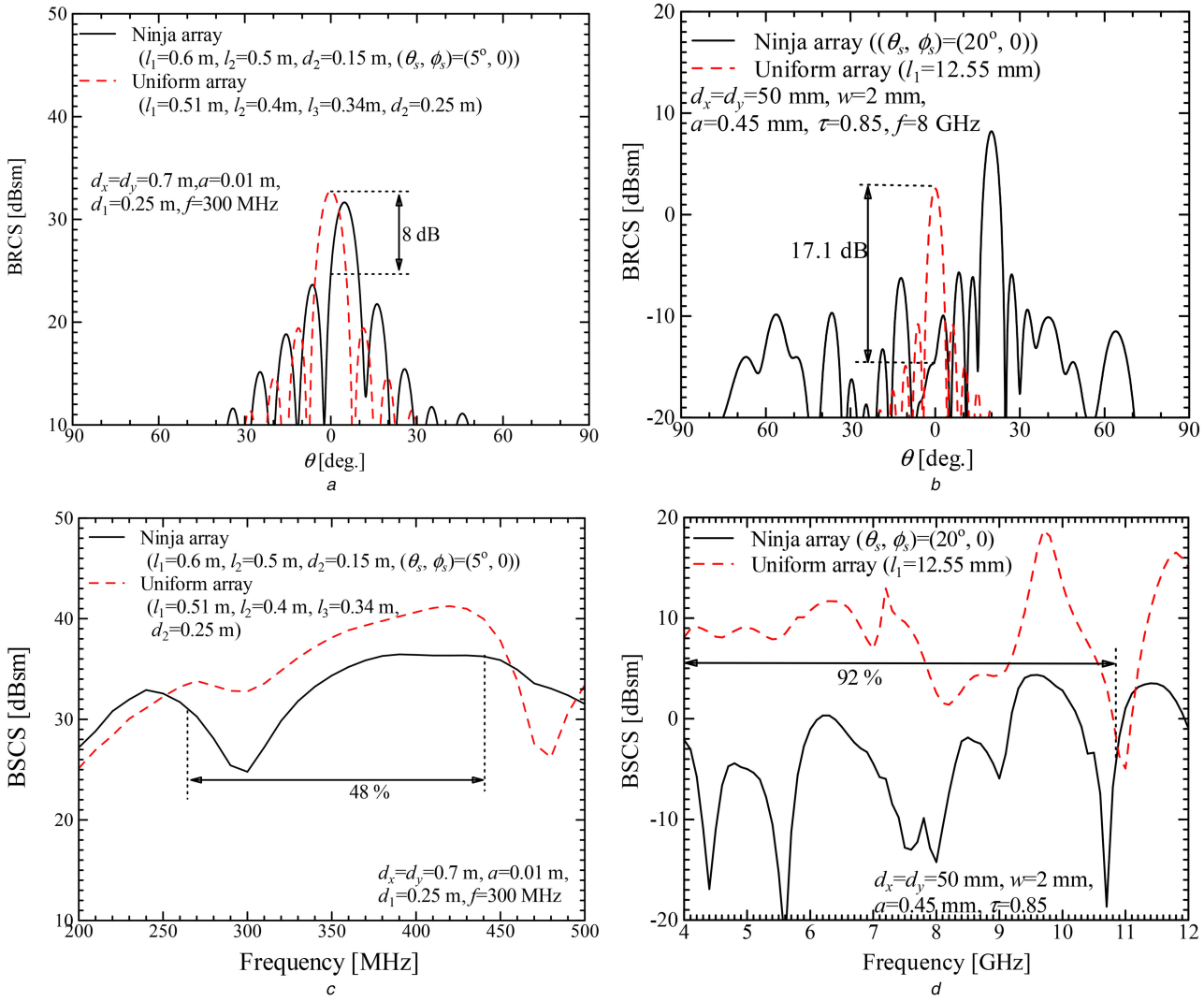

Fig. 6 *Scattering performance of designed* 10×10 *uniform and Ninja array antennas*

(a) BRCSs of uniform and Ninja array antennas with Yagi-Uda elements (*xz*-plane, E_ϕ, normal incidence), ***(b)*** BRCSs of uniform and Ninja array antennas with LPDA elements (*xz*-plane, E_ϕ, normal incidence), ***(c)*** Bandwidth of BSCSs of uniform and Ninja arrays antennas with Yagi-Uda elements (*xz*-plane, E_ϕ, normal incidence), ***(d)*** Bandwidth of BSCSs of uniform and Ninja array antennas with LPDA elements (*xz*-plane, E_ϕ, normal incidence)

sidelobe level increases abruptly. Here, the maximum beam scanning range is defined as a range over which the drop of the actual gain from its peak is <3 dB. The maximum beam scanning range is $\pm 60^\circ$ and $\pm 30^\circ$ for the Ninja array antenna with the Yagi-Uda element and the LPDA element, respectively. According to relatively wide array spacing, the maximum beam scanning range of the Ninja array antenna with the LPDA element ($d_x/2 = d_y/2 = 0.67\lambda$ at 8 GHz) is smaller than that with the Yagi-Uda element ($d_x/2 = d_y/2 = 0.33\lambda$ at 300 MHz).

4 Conclusion

In this paper, a Ninja array antenna which is a novel low backscattering phased array antenna has been proposed. The Ninja array antenna is composed of a lot of non-identical array elements and is designed in the same manner as the design of reflectarrays. As a result, the Ninja array antenna shows relatively low backscattering in its operating frequency band compared with a uniform array antenna which is composed of identical array elements. A novel method for computing an excitation vector has been proposed for the Ninja array antenna. The proposed method is based on array element patterns and resultant excitation vector makes the Ninja array antenna to form a main beam directed to the desired direction. Numerical simulation was performed and Ninja array antennas which are composed of single/multi-mode elements were designed. Low backscattering performance and beam scanning capability of these Ninja array antennas have been demonstrated.

This paper only focused on a concept of a low backscattering phased array antenna itself and a lot of problems to be discussed is still remaining. For example, a phased array antenna has a lot of microwave components such as phase shifter, amplifier, and cables that has not been dealt with in this paper. These microwave components may have negative impacts on the performance of the Ninja array antenna. The performance of the Ninja array antenna including these microwave components is expected to be studied. Although our study has demonstrated the performance of the Ninja array antenna numerically, an experimental study of the Ninja array antenna is also expected. The Ninja array antenna should be fabricated and its scattering/radiation performance will be measured in future.

5 Acknowledgments

We would like to thank staffs in Cyberscience Center, Tohoku University, for their helpful advices. This work was financially supported by JSPS KAKENHI grant number 25420394 and 26820137, and JSPS Postdoctral Fellowships for Research Abroad.

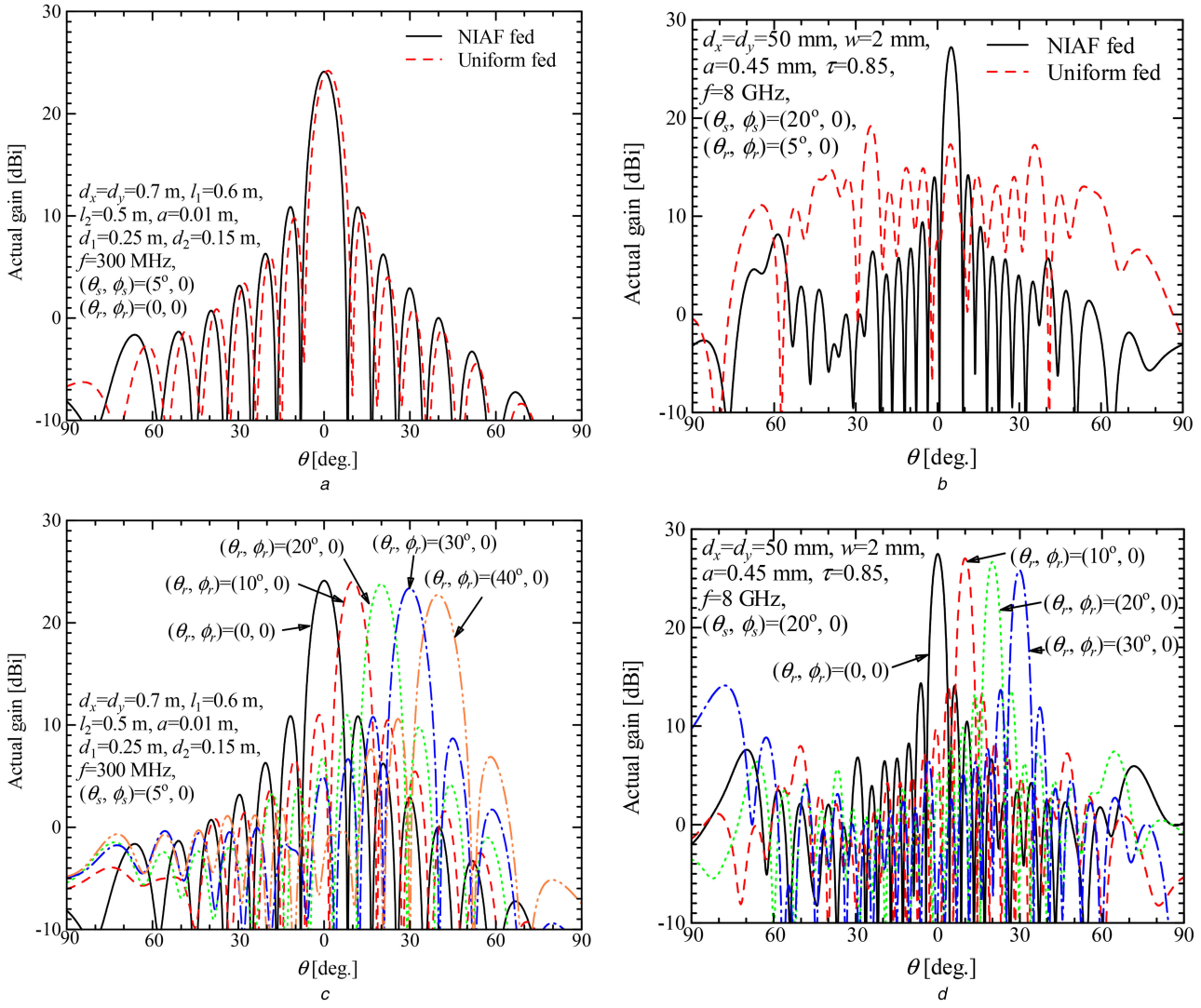

Fig. 7 *Beam scanning performance of the proposed excitation method on* 10×10 *Ninja array antennas*

(a) Actual gain patterns of a Ninja array antenna with Yagi-Uda elements (*xz*-plane, E_ϕ), ***(b)*** Actual gain patterns of a Ninja array antenna with LPDA elements (*xz*-plane, E_ϕ), ***(c)*** Beam scanning performance of a Ninja array antenna with Yagi-Uda elements (*xz*-plane, E_ϕ), ***(d)*** Beam scanning performance of a Ninja array antenna with LPDA elements (*xz*-plane, E_ϕ)

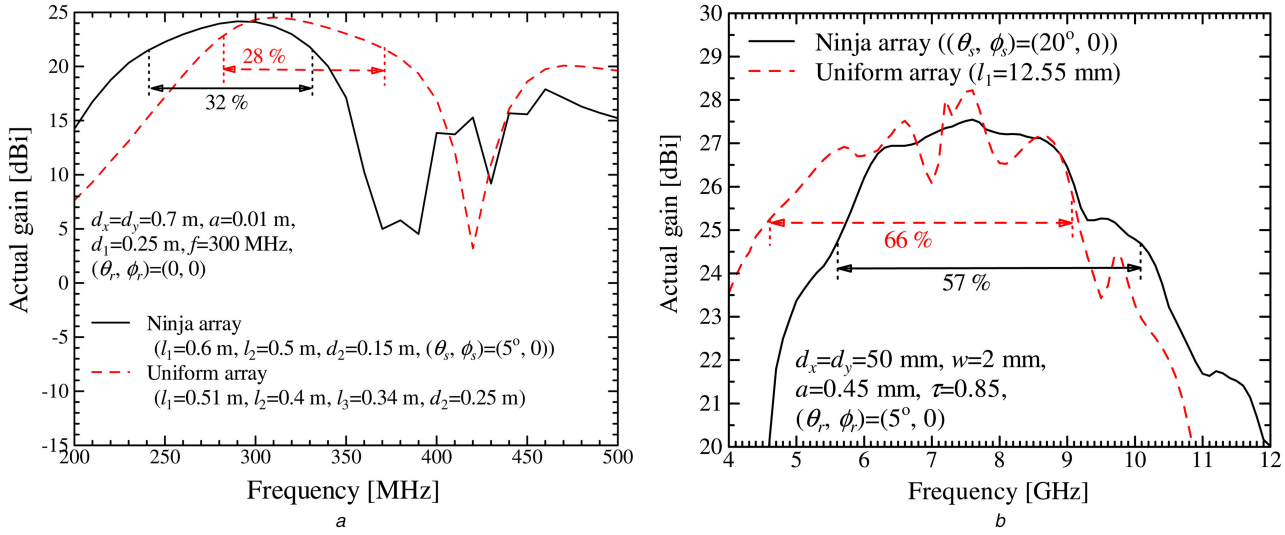

Fig. 8 *Actual gain of designed* 10×10 *uniform and Ninja array antennas over frequency domain*

(a) Bandwidth of actual gain of uniform and Ninja array antennas with Yagi-Uda elements (*xz*-plane, E_ϕ), ***(b)*** Bandwidth of actual gain of uniform and Ninja array antennas with LPDA elements (*xz*-plane, E_ϕ)

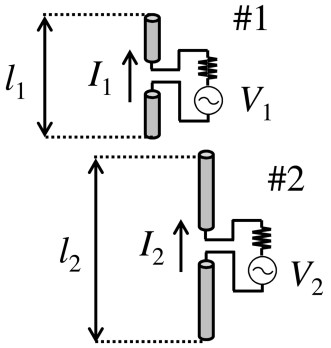

Fig. 9 *Beam scanning capability of designed* 10×10 *uniform and Ninja array antennas in H-plane*

(a) Mainlobe and the maximum sidelobe levels of uniform and Ninja array antennas with Yagi-Uda elements (*xz*-plane, E_ϕ), ***(b)*** Mainlobe and the maximum sidelobe levels of uniform and Ninja array antennas with LPDA elements (*xz*-plane, E_ϕ)

6 References

[1] Hansen, R.C.: '*Phased array antennas*' (John Wiley & Sons, 1998)

[2] Mailloux, R.J.: '*Phased array antenna handbook*' (Artech House, Boston, London, 1994)

[3] Konishi, Y.: 'Phased array antennas', *IEICE Trans. Commun.*, 2003, **E86-B**, (3), pp. 954–967

[4] Munk, B.A.: '*Frequency selective surfaces theory and design*' (John Wiley & Sons, 2000)

[5] Munk, B.A.: '*Finite antenna arrays and FSS*' (John Wiley & Sons, 2003)

[6] Inasawa, Y., Nishimura, T., Tsuruta, J., *et al.*: 'Using conducting wire at A-sandwich junctions to improve the transmission performance of radomes', *IEICE Trans. Commun.*, 2008, **E91-B**, (8), pp. 2764–2767

[7] Lin, B.-Q., Li, F., Zheng, Q.-R., *et al.*: 'Design and simulation of a miniature thick-screen frequency selective surface radome', *IEEE Wirel. Propag. Lett.*, 2009, **8**, pp. 1065–1068

[8] Costa, F., Monorchio, A.: 'A frequency selective radome with wideband absorbing properties', *IEEE Trans. Antennas Propag.*, 2012, **60**, (6), pp. 2740–2747

[9] Hashimoto, O., Abe, T., Satake, R., *et al.*: 'Design and manufacturing of resistive-sheet type wave absorber at 60 GHz frequency band', *IEICE Trans. Commun.*, 1995, **E78-B**, (2), pp. 246–252

[10] Kurihara, H., Saito, T., Tanizawa, K., *et al.*: 'Investigation of EM wave absorbers by using resistive film with capacitive reactance', *IEICE Trans. Electron.*, 2005, **E88-C**, (11), pp. 2156–2162

[11] Zhao, Y., Liu, J., Song, Z., *et al.*: 'Microstructure design method for multineedle whisker radar absorbing material', *IEEE Antennas Wirel. Propag. Lett.*, 2016, **15**, pp. 1163–1166

[12] Bai, B., Li, X., Xu, J., *et al.*: 'Reflections of electromagnetic waves obliquely incident on a multilayer stealth structure with plasma and radar absorbing material', *IEEE Trans. Plasma Sci.*, 2015, **43**, (8), pp. 2588–2596

[13] Song, Y.-C., Ding, J., Guo, C.-J., *et al.*: 'Ultra-broadband backscatter radar cross section reduction based on polarization-insensitive metasurface', *IEEE Antennas Wirel. Propag. Lett.*, 2016, **15**, pp. 329–331

[14] Hou, Y.-C., Liao, W.-J., Tsai, C.-C., *et al.*: 'Planar multilayer structure for broadband broad-angle RCS reduction', *IEEE Trans. Antennas Propag.*, 2016, **64**, (5), pp. 1859–1867

[15] Berry, D.G., Malech, R.G., Kennedy, W.A.: 'The reflectarray antenna', *IEEE Trans. Antennas Propag.*, 1963, **11**, (6), pp. 645–651

[16] Huang, J.: 'Analysis of a microstrip reflectarray antenna for microspacecraft applications'. TDA Progress Report 42-120, February 1995, pp. 153–173

[17] Huang, J., Encinar, J.A.: '*Refrectarray antennas*' (John Wiley and Sons, 2008)

[18] Venneri, F., Angiulli, G., Di Massa, G.: 'Design of microstrip reflectarray using data from isolated patch analysis', *Microw. Opt. Technol. Lett.*, 2002, **34**, (6), pp. 411–414

[19] Milon, M.-A., Cadoret, D., Gillard, R., *et al.*: 'Surrounded-element' approach for the simulation of reflectarray radiating cells', *IET Microw. Antennas Propag.*, 2007, **1**, (2), pp. 289–293

[20] Yann, C., Loison, R., Gillard, R., *et al.*: 'A new approach combining surrounded-element and compression methods for analyzing reconfigurable reflectarray antennas', *IEEE Trans. Antennas Propag.*, 2012, **60**, (7), pp. 3215–3221

[21] Wan, C., Encinar, J.A.: 'Efficient computation of generalized scattering matrix for analyzing multilayered periodic structures', *IEEE Trans. Antennas Propag.*, 1995, **43**, (11), pp. 1233–1242

[22] Li, L., Chen, Q., Yuan, Q., *et al.*: 'Novel broadband planar reflectarray with parasitic dipoles for wireless communication applications', *IEEE Antennas Wirel. Propag. Lett.*, 2009, **8**, pp. 881–885

[23] Li, L., Chen, Q., Yuan, Q., *et al.*: 'Frequency selective reflectarray using crossed-dipole elements with square loops for wireless communication applications', *IEEE Trans. Antennas Propag.*, 2011, **59**, (1), pp. 89–99

[24] Harrington, R.F.: '*Field computation by moment methods*' (Macmillan, New York, 1968)

[25] Richmond, J.H., Geary, N.H.: 'Mutual impedance of nonplanar-skew sinusoidal dipoles', *IEEE Trans. Antennas Propag.*, 1975, **23**, (3), pp. 412–414

[26] Yagi, H., Uda, S.: 'Projector of the sharpest beam of electric waves', *Proc. Imperial Acad. Japan*, 1926, **2**, (2), pp. 49–52

[27] Mushiake, Y.: 'Self-complementary antennas', *IEEE Antennas Propag. Mag.*, 1992, **34**, (6), pp. 23–29

[28] Duhamel, R.H., Isbell, D.E.: 'Broadband logarithmically periodic antenna structure'. IRE National Convention Record, pt.1, March 1957, pp. 119–128

[29] Isbell, D.E.: 'Log periodic dipole arrays', *IRE Trans. Antennas Propag.*, 1960, **AP-8**, (3), pp. 260–267

[30] Yokokawa, K., Konno, K., Chen, Q.: 'Scattering performance of log-periodic dipole array', *IEEE Antennas Wirel. Propag. Lett.*, 2017, **16**, pp. 740–743

[31] Ito, H., Konno, K., Sato, H., *et al.*: 'Wideband scattering performance of reflectarray using log-periodic dipole array', *IEEE Antennas Wirel. Propag. Lett.*, 2017, **16**, pp. 1305–1308

7 Appendix

In order to explain the proposed excitation method clearly, how to obtain an excitation vector for a Ninja array antenna with two small non-identical dipole elements ($N = M = 2$) is described as an example. Geometry of the Ninja array antenna is shown in Fig. 10 and the reference element is #1 (i.e. $l_1 = l_R$). At first, array element currents are obtained via following 2×2 matrix equations

$$\boldsymbol{I}_1 = \begin{bmatrix} Z_{11} & Z_{12} \\ Z_{21} & Z_{22} \end{bmatrix}^{-1} \begin{bmatrix} 1 \\ 0 \end{bmatrix} \tag{8}$$

$$\boldsymbol{I}_2 = \begin{bmatrix} Z_{11} & Z_{12} \\ Z_{21} & Z_{22} \end{bmatrix}^{-1} \begin{bmatrix} 0 \\ 1 \end{bmatrix}. \tag{9}$$

After that, array element patterns corresponding to the array element currents $\boldsymbol{I}_1$ and $\boldsymbol{I}_2$ are obtained for a specific (θ_r, ϕ_r), respectively. Finally, the NIAFs $C_1 (= 1)$ and C_2 are obtained via (4) and excitation vector for the Ninja array antenna is given as $\boldsymbol{V} = [C_1, C_2]$.

For example, the NIAFs for the Ninja array antenna ($l_1 = l_R = 0.2\lambda$, $l_2 = 0.1\lambda$, radius $a = 0.001\lambda$, array spacing is 0.6λ, and side-by-side) are obtained as follows. According to Richmond's MoM [25], $Z_{11} = 58.33 - \mathrm{j}588.6$, $Z_{12} = Z_{21} = -1.24 - \mathrm{j}0.96$, $Z_{22} = 52 - \mathrm{j}1082.2$ for the Ninja array antenna including $50\,\Omega$ load. Array element currents are $\boldsymbol{I}_1 = [1.67 \times 10^{-4} + \mathrm{j}1.68 \times 10^{-3}, -2.14 \times 10^{-6} - \mathrm{j}1.2 \times 10^{-6}]$, $\boldsymbol{I}_2 = [-2.14 \times 10^{-6} - \mathrm{j}1.2 \times 10^{-6}, 4.43 \times 10^{-5} + \mathrm{j}9.22 \times 10^{-4}]$. The resultant NIAFs for the Ninja array antenna are $C_1 = 1$, $C_2 = 3.49 - \mathrm{j}1.41$ when $(\theta_r, \phi_r) = (5^\circ, 0)$.

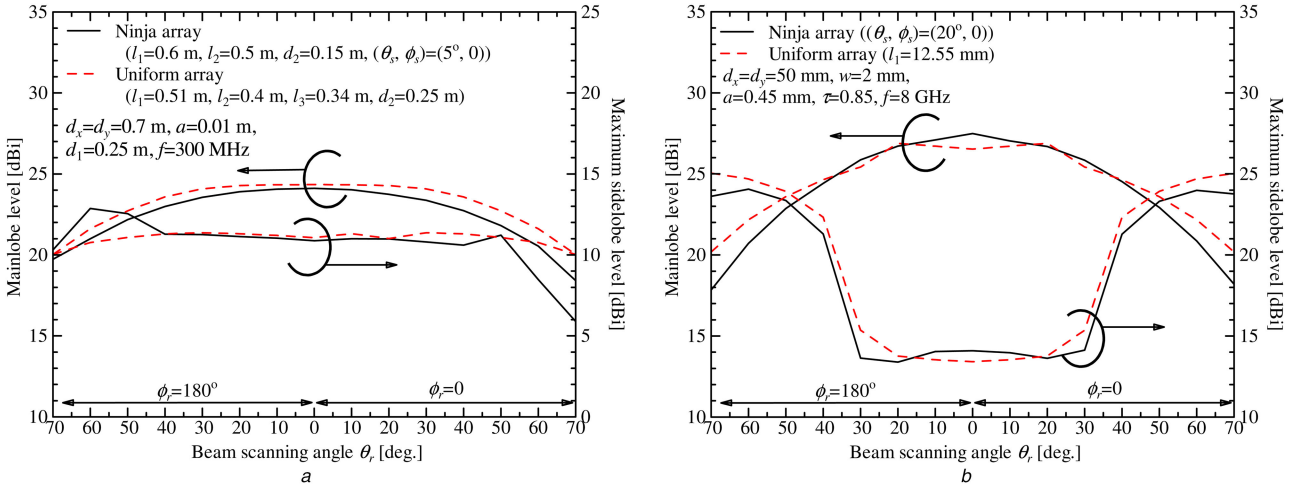

Fig. 10 *Ninja array antenna with two small non-identical dipole elements*